Int. J. Electrochem. Sci., 2 (**2007**) 478 - 487

International Journal of ELECTROCHEMICAL SCIENCE
www.electrochemsci.org

Synthesis and Electrochemical Characterization of Novel Category $Si_{3-x}M_xN_4$ (M= Co, Ni, Fe) Anodes for Rechargeable Lithium Batteries

N.Kalaiselvi

Central Electrochemical Research Institute, Karaikudi 630 006, India
E-mail: kalakanth2@yahoo.com

Received: 2 April 2007 / *Accepted:* 13 May 2007 / *Published:* 1 June 2007

A novel category Si_3N_4 anode and a series of doped derivatives of silicon nitride with a general formula $Si_{3-x}M_xN_4$ (M= Co, Ni and Fe) were synthesized, characterized and exploited as possible alternative anodes for rechargeable lithium batteries through the present study. The compound Si_3N_4 exhibited inferior capacity (~ 100 mAh/g) compared to the carbonaceous and lithiated nitride anodes. On the other hand, the $Si_{3-x}M_xN_4$ compounds (M = Co, Ni, Fe) qualified themselves as better anodes with a specific capacity of at least 130 ~ 470 mAh/g, and lesser capacity fade (< 20 %) after 50 cycles. Particularly, $Si_{3-x}Fe_xN_4$ anode showed the highest specific capacity of 470 mAh/g, wheras the rest of the anodes, viz., Si_3N_4 and $Si_{3-x}M_xN_4$ (M= Co, Ni) exhibited better capacity retention upon cycling. The lowest average oxidation number and the higher ionic radius of Fe compared to Co and Ni metals are believed to be responsible for the improved specific capacity values and the excellent coulumbic efficiency (99%) of $Si_{3-x}Fe_xN_4$ anodes, via. restricted formation of passivating surface film.

Keywords: silicon metal nitride; lithium battery anode; capacity; cycleability; coulumbic efficiency

1. INTRODUCTION

Lithium-ion batteries, which are based on the intercalation process of lithium in to carbonaceous anodes, perform well in terms of cycleability. But they suffer from low energy density problems, due to which attempts to improve the capacity and energy density of lithium-ion systems become highly essential for their wider acceptance towards multifarious applications. Recently, ternary lithium metal nitrides of both antiflourite [$Li_{2-n}MN_n$ type] and hexagonal structure [Li_3N type] were found to exhibit good electrochemical cycling behavior [1-4] and in particular, the hexagonal Li_3N category, which is composed of $Li_2^+N^{3-}$ layers [5] were found to exhibit a comparatively better capacity [6]. Subsequently, $Li_{3-x}M_xN$ [M= Co, Ni, Fe, …] anodes gained paramount importance [7] and so the electrochemical behavior of lithium nitride anodes were studied with respect to different

electrolytes [8] in order to understand the degradation mechanism of the same in a detailed manner. However, requirement of stringent synthesis conditions to prepare $Li_{3-x}M_xN$ anodes and their poor cycle life performance, despite the addition of Fe as dopant [9] remain as unsolved problems till date [9].

Therefore, a newer approach to examine and explore the possibility of employing novel category silicated transition metal nitride anodes is sought in the present investigation. Taking in to consideration of the fact that enhanced lithium-ion migration and creation of lithium defects are possible in lithium-ion systems, via. decreasing Li-N interaction [10,11] (through hydrogen doping), the present study aims at the exploitation of Si_3N_4 and $Si_{3-x}M_xN_4$ [M= Co, Ni, Fe] anodes, primarily with a view to reduce the Li-N interaction, via. formation of silicon defective electrode matrix and to circumvent the moisture sensitivity problems related to the synthesis of lithium nitride anodes possibly. In particular, the study deals with the synthesis, characterization and electrochemical evaluation of Si_3N_4 and $Si_{3-x}M_xN_4$ [M= Co, Ni, Fe] category anodes individually in order to understand the effect of individual dopants in modifying the electrochemical characteristics.

2. EXPERIMENTAL PART

2.1 Synthesis procedure

A mixture of Si_3N_4 and respective metal powders, viz., cobalt, nickel or iron (x = 0.4) was ground in an agate mortar for about 30 minutes, pelletized by applying a pressure of 25 MPa in a hydraulic press and the pellets were heat treated initially to 300 ºC for 24 h. in nitrogen atmosphere. Subsequently, intermittent grinding was given after every 8h. interval to re-assure intimate and homogenous mixing of the ingredients during and/or after the process of low calcination treatment. Further, the powders were subjected to high temperature calcination at 800 ºC [3 h.] in the nitrogen gas atmosphere and the final products were recovered as ultra fine powders from the furnace. Ultimately the powders were ground again and subjected to characterization studies such as PXRD, SEM, charge-discharge (at a constant current rate) and cyclic voltammetry analysis.

2.2 Structural and morphological characterization

Phase characterization was done by powder X-ray diffraction technique on a Philips 1830 X-ray diffractometer using Ni filtered Cu-K_α radiation (λ = 1.5406 Å) in the 2θ range of 10 ~ 120 ^{o} at a scan rate of 0.1 ^{o}/sec. Surface morphology of the particles was examined through SEM images obtained from Jeol S-3000 H Scanning Electron microscope. Charge-discharge studies were carried out using MACCOR charge-discharge cycle life tester and the CV studies were performed with IM-6 Electrochemical Impedance Spectrometer.

2.3 Electrochemical characterization

The anode electrode was prepared by coating a slurry that contains a mixture of synthesized nitride powder (80 % by weight), carbon (10 %) and PVdF binder (10 %) over a copper foil and the

details are mentioned elsewhere [12]. The moisture controlled electrodes were used against a lithium foil of thickness 120 µm and an electrolyte of 1:1 v/v EC:DEC dissolved in 1M $LiPF_6$. A polypropylene separator (Asahi) of 20 µm thickness with 40 % porosity was used. The fabricated pouch cells were kept in the dry room for one day (aging process) before subjected to charge-discharge analysis.

3. RESULTS AND DISCUSSION

3.1 Structural results - PXRD studies

The PXRD pattern recorded for the parent compound Si_3N_4 and the dopant metals selected for the present study, namely Co, Ni and Fe are depicted in Figs.1a-d respectively. The observed peak pattern of Si_3N_4 compound (Fig.1a) was found to have a perfect match with the standard JCPDS pattern of trigonal structure with *p31c* space group. Therefore, it is understood that Si_3N_4 compound has a trigonal structure (space group: *p31c*) [13], wherein possibilities to partially accommodate the mentioned dopants for Si appears to be appreciable [1].

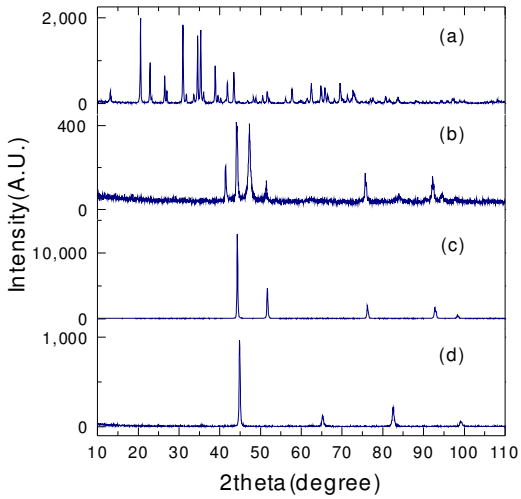

Figure 1. XRD patterns of raw materials; (a) Si_3N_4, (b) Co, (c) Ni, (d) Fe powder

Eventually, the effect of incorporated dopant(s) are expected to change or enhance the intensity of the basic peaks observed for Si_3N_4 compound, along with the appearance of newer and characteristic peaks of dopant metal(s) at appropriate positions in the final products. Interestingly, the same has been observed with the present set of newly identified $Si_{3-x}M_xN_4$ compounds (Figs.2b-d), without changing the basic bragg pattern of the parent Si_3N_4 compound. Thus it is implied that the dopants (Co, Ni or Fe) have successfully been incorporated in to the trigonal matrix of Si_3N_4 compound. Also, it is understood that the system Si_3N_4 forms a solid solution wherein the presence of Si in the Si_3N_4

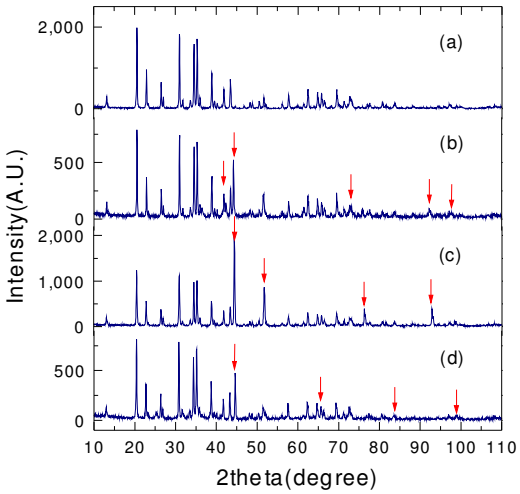

Figure 2. XRD patterns of $Si_{3-x}M_xN_4$ compounds; (a) Si_3N_4, (b) M=Co, (c) M=Ni, (d) M=Fe

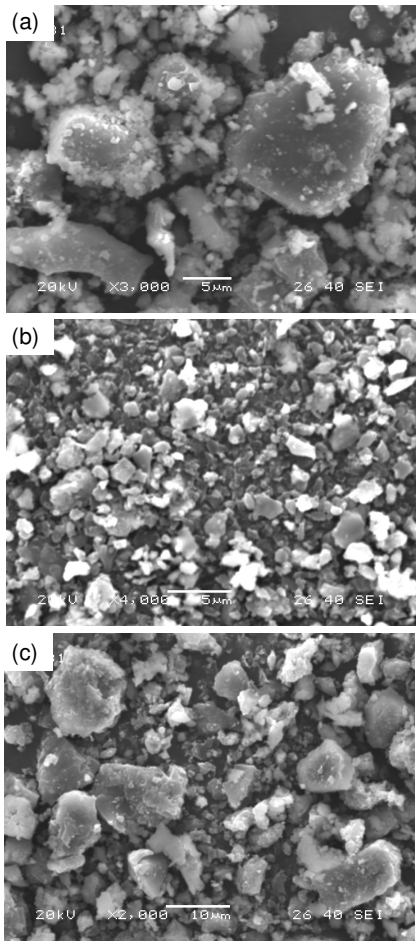

Figure 3. SEM photographs of $Si_{3-x}M_xN_4$ compounds; (a) M=Co, (b) M=Ni, (c) M=Fe

structure has partially been substituted by Co, Ni or Fe. It is noteworthy that the upper solubility limit of the system is yet to be identified and the present study is restricted, especially with the preliminary understanding of possible existence of solid solutions of $Si_{3-x}M_xN_4$ compounds, with respect to the mentioned limit of dopant concentration.

Interestingly, no extra peaks were identified in the PXRD pattern recorded for the entire set of $Si_{3-x}M_xN_4$ compounds (Figs.2b-d), which is an indication of single phase formation or the phase purity of final products. Also, the bragg peaks exhibited by Si_3N_4 and the solid solutions of $Si_{3-x}M_xN_4$ [M = Co, Ni, Fe] type were found to be sharp and intense in nature, thus accounting for the better crystallinity of the synthesized products.

3.2 Morphological results - SEM analysis

SEM images captured under × 2,000 ~ × 4,000 magnification for $Si_{3-x}M_xN_4$ [M = Co, Ni, Fe] compounds are appended in Figs. 3a-c. The metal-doped silicon nitrides were found to contain un agglomerated spherical grains of clearly seen crystal boundaries, as evident from the figure. However, presence of individual grains with a different order of distribution was observed with the cobalt /nickel/iron doped silicon nitrides. Therefore, it is understood that despite the deployment of similar calcination conditions towards the synthesis of $Si_{3-x}M_xN_4$ compounds [M = Co, Ni, Fe], the surface morphology of the final products vary as a function of inherent nature of the individual dopant. However, absence of agglomeration and the presence of independent and grain growth controlled particles with confined crystal facets (Figs.3a-c) are in support of both structurally and electrochemically favored surface morphology features of the $Si_{3-x}M_xN_4$ [M = Co, Ni, Fe] compounds. Therefore, the presence of sub-micron sized (5 ~ 10 μm) particles obtained from the specially adopted intermittent grinding and the gradually enhanced and/or reduced furnace temperature (observed towards the calcination process) is found to yield silicon metal nitrides with preferred surface morphology [14].

3.3 *Electrochemical characterisation results*

Based on the available reports of Li_3N and the $Li_{3-x}Co_xN$ anodes [1,3,8], it may appear to be difficult to obtain the metal-doped silicon nitrides with perfect stoichiometric composition. While considering the stable existence of M ions in the ionic crystal, $Si_{3-x}M_xN_4$ compounds seem to have some sort of Si defect or distribution, which may not be ignored. Consequently, such a behavior of Si is expected to result in the formation of additional vacant sites in the basic matrix of the Si_3N_4 compound, which in turn may act presumably as lithium intercalation/red-ox centers. Based on these grounds, the synthesized $Si_{3-x}M_xN_4$ compounds are expected to exhibit possible anode performance characteristics against lithium metal.

3.3.1 Charge-discharge studies

To understand the effect of individual dopants in improving the electrochemical properties of Si_3N_4 anodes, a series of Li | Si_3N_4 , Li | $Si_{3-x}Co_xN_4$, Li | $Si_{3-x}Ni_xN_4$, Li | $Si_{3-x}Fe_xN_4$ cells were

fabricated and subjected to charge-discharge studies at a constant (C/10) current rate. The charge-discharge curves obtained for Si_3N_4 and $Si_{3-x}M_xN_4$compounds cycled between 0 ~ 3.3 V are furnished in Figs. 4a-d. Initially, the voltage of Si_3N_4 drops suddenly (up to 1.2 V), followed by a small plateau (0.7 V), and finally the cell voltage decreases (Fig.4a) gradually. Such type of discharge behavior of Si_3N_4 anode may be attributed to the combined effects of change of structure from crystalline to amorphous state, and to a possible change of surface morphology [9], presumably due to the formation of protective surface film over the anode electrode. Despite the lower initial discharge capacity value (~100mAh/g) of Si_3N_4 anode, the subsequent capacity values (from second cycle) were found to increase upon extended cycling, which may be attributed to the electrochemically driven size confinement of the particles, otherwise known as the electrochemical grinding of electrode material to form nano particles [15]. The capacity loss was found to get reduced to the extent of 15 % (from 55 %) after 10 cycles, thus showed marked improvement in the coulumbic efficiency upon cycling.

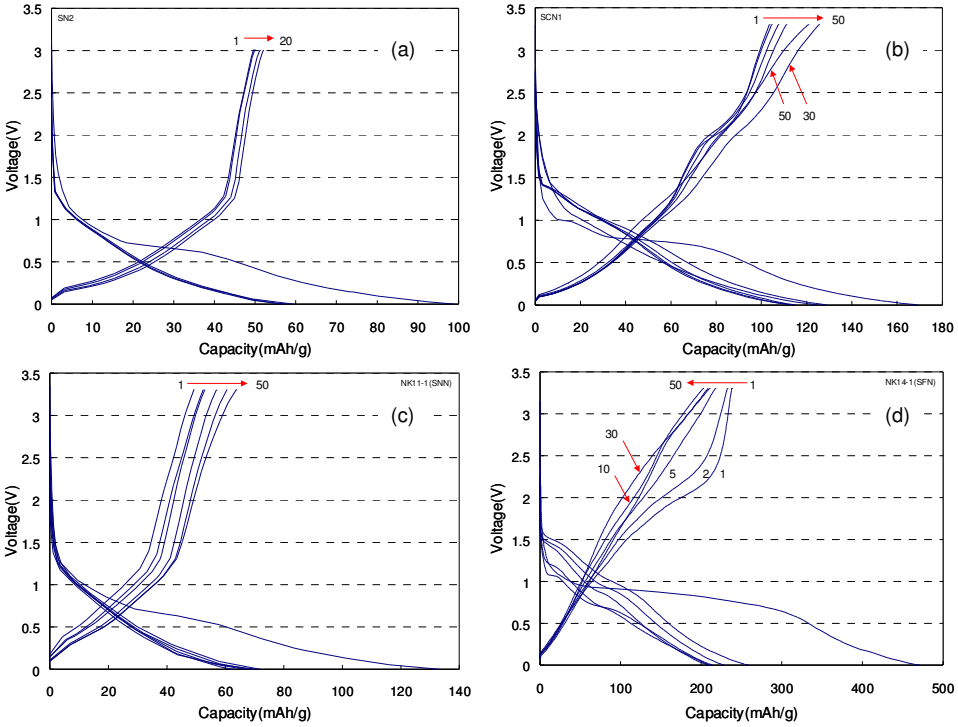

Figure 4. Voltage profiles of Li | $Si_{3-x}M_xN_4$ cells; (a) Si_3N_4, (b) M=Co, (c) M=Ni, (d) M=Fe

Figs. 4(b)-(d) represent the charge-discharge behaviors of $Si_{3-x}M_xN_4$ compounds with M = Co, Ni, Fe respectively. The small plateau region of the initial discharge curve exhibited by $Si_{3-x}M_xN_4$ [M = Co, Ni, Fe] compounds substantiates the involvement of two phases [9] reaction during the intercalation/de-intercalation process. i.e., the structure of $Si_{3-x}M_xN_4$ [M = Co, Ni, Fe] compounds changes from crystalline to amorphous phase in the first cycle and the amorphous state is expected to be maintained upon extended cycling. Also, the potential plateau of $Si_{3-x}M_xN_4$ compounds were observed below 1.0 V (~ 0.7 – 0.9 V), which is much lower than the Li_3N / $Li_{3-x}M_xN$ type of anodes [1,3], thus qualifying themselves as better anodes. More interestingly, the capacity of $Si_{3-x}M_xN_4$ [M = Co, Ni, Fe] compounds was found to increase gradually from second cycle onwards, and thus resulted

in lower capacity fade upon cycling. It is believed that the maintenance of amorphous phase upon extended cycling attributes to the reduced capacity fade behavior of $Si_{3-x}M_xN_4$ anodes.

The capacity of $Si_{3-x}Co_xN_4$ compound increased gradually up to 40 cycles (~ 128 mAh/g) and a slightly reduced capacity has further been observed up to 50 cycles (~ 126 mAh/g). However, the capacity of $Si_{3-x}Co_xN_4$ anode after 50 cycles is found to be higher (Fig.4b) than the initial charging capacity (~ 105 mAh/g) of Si_3N_4 anode. Incidentally, a possible and a fundamental rearrangement of elements that is concerned with the short-range ordering of amorphous state of silicon metal nitride derivatives is expected to occur [7], which is responsible for the increase in capacity observed upon cycling.

Table 1. Comparison of electrochemical behavior of $Si_{3-x}M_xN_4$ anodes

	Si_3N_4			$Si_{3-x}Co_xN_4$			$Si_{3-x}Ni_xN_4$			$Si_{3-x}Fe_xN_4$		
Cycle	Qc	Qd	Qe	Qc	Qd	Qe	Qc	Qd	Qe	Qc	Qd	Qe
1	98.6	52.7	53.4	169.3	105.0	62.0	132.8	53.5	40.3	470.6	237.7	50.5
10	56.7	54.6	96.3	113.5	110.7	97.5	66.7	63.5	95.2	212.9	206.4	96.9
20	56.7	55.4	97.7	120.7	118.7	98.3	65.7	64.1	97.6	201.4	199.8	99.2
30	-	-	-	128.3	125.7	98.0	67.1	66.1	98.5	210.0	206.6	98.4
40	-	-	-	128.5	125.9	98.0	65.3	64.5	98.8	212.3	210.5	99.1
50	-	-	-	126.2	122.6	97.1	70.7	69.9	98.9	213.6	210.9	98.7

*Qc : Charge capacity(mAh/g) , Qd : Discharge capacity(mAh/g), Qe : Coulumbic efficiency(%, nQd/nQc)

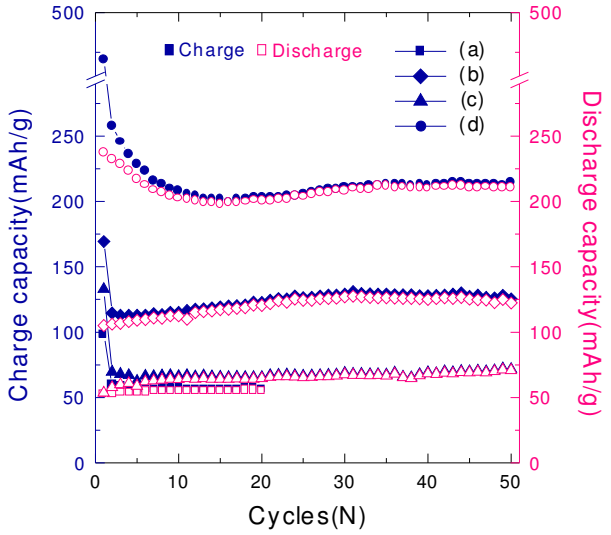

Figure 5. Capacity comparison of Li | $Si_{3-x}M_xN_4$ cells; (a) Si_3N_4, (b) M=Co, (c) M=Ni, (d) M=Fe

Similar to the case of Si_3N_4 and $Si_{3-x}Co_xN_4$ anodes, $Si_{3-x}M_xN_4$ compounds with M = Ni and Fe (Figs.4c &d) also exhibited plateau below 1.0 V and the magnitude of plateau (at 0.8 ~ 0.9 V) was found to be larger for $Si_{3-x}Fe_xN_4$ compound. Basically, $Si_{3-x}Ni_xN_4$ compound exhibited an initial discharge capacity value of ~ 133 mAh/g, a value considerably higher than the parent Si_3N_4 compound and slightly lower than that of $Si_{3-x}Co_xN_4$ anode. It is noteworthy that such a lower specific capacity value has already been reported for nickel doped Li_3N compounds [7] and so the initial lower capacity value of $Si_{3-x}Ni_xN_4$ compound need not be considered as an adverse effect of nickel dopant. Probably, the short-range ordering with respect to the amorphous state of $Si_{3-x}Ni_xN_4$ compound after lithium extraction follows a different pattern from that of cobalt system [7], and thereby results in lesser initial specific capacity values. On the other hand, $Si_{3-x}Ni_xN_4$ compound showed increasing capacity values up to 50 cycles, thus resulted in the minimized irreversible capacity loss values upon cycling (Fig.4c).

Interestingly, $Si_{3-x}Fe_xN_4$ compound exhibited the highest discharge capacity of ~ 470 mAh/g, (Fig.4d) compared to both the un-doped and doped derivatives of Si_3N_4 anode. On the other hand, unlike the case of Co and Ni, Fe dopant has not showed any markedly enhanced capacity values upon extended cycling compared to the initial charge/discharge capacity values. However, the capacity after 50 cycles was found to be 210 mAh/g, which is about 2.5 times higher than Si_3N_4 and about 1.5 times higher than the initial capacity values of $Si_{3-x}M_xN_4$ compounds with M = Co or Ni. The lowest average oxidation number and the highest ionic radius of Fe compared to Co and Ni metals are believed to be responsible for the considerably improved specific capacity values of $Si_{3-x}Fe_xN_4$ anodes, via. restricted formation of passivating surface film.

A comparison of charge-discharge behavior of $Si_{3-x}M_xN_4$ compounds [M = Co, Ni, Fe] in terms of specific capacity values at regular intervals and columbic efficiency is displayed in Table 1. From the table, it is evident that the coulumbic efficiency of all the select category silicon nitride based anodes are excellent, despite the unavoidable initial irreversible capacity loss problem. Further, it is understood that the $Si_{3-x}Fe_xN_4$ anode exhibits the highest capacity and the rest of the Si_3N_4 and $Si_{3-x}M_xN_4$ [M = Co, Ni] anodes possess better capacity retention capability, as obvious from Fig.5 also. Thus, the difference in the electrochemical behavior of $Si_{3-x}M_xN_4$ compounds with M = Co, Ni, Fe may very well be understood as a function of basic differences observed with respect to the surface morphology patterns and the inherent nature of the individual metal dopants. Similarly, the effect of change of crystalline to amorphous phase and the subsequent electrochemical grinding of sub-micron sized particles upon cycling are considered to improve the cycleability of all the Si_3N_4 and $Si_{3-x}M_xN_4$ [M = Co, Ni] anodes, irrespective of the type and nature of the dopants.

3.3.2 Cyclic voltammetry studies

In order to examine the fact that whether lithium ion is inserted in to the active material and extracted from it, CV analysis was carried out at a slow scan rate of 1 mV/sec. The recorded CV patterns of $Si_{3-x}M_xN_4$ compounds with M = Co, Ni, Fe are displayed in Figs. 6a-c.

Basically, all the $Si_{3-x}M_xN_4$ [M = Co, Ni, Fe] compounds exhibited two main peaks, corresponding to the involvement of two main reactions in each process.

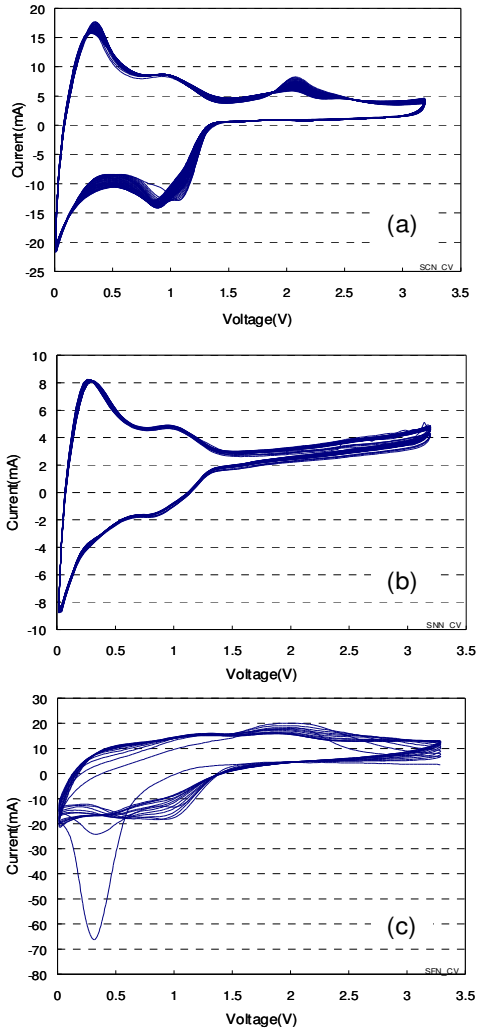

Figure 6. Cyclic voltammograms of Li | $Si_{3-x}M_xN_4$ cells; (a) M=Co, (b) M=Ni, (c) M=Fe

This type of reactions in the charge or discharge curves are generally reported to have something to do with the site of existence of lithium ion [9], which is beyond the scope of the present study. However, the observed CV features of $Si_{3-x}M_xN_4$ compounds agree very well with the reported behavior of similarly studied Li_3N category anodes [16] and hence the cyclic reversibility of $Si_{3-x}M_xN_4$ derivatives is substantiated.

Further, the CV patterns of $Si_{3-x}M_xN_4$ (M=Co,Ni) compounds showed no considerable shift (Figs.6a&b) in peak positions (up to 50 cycles), thus substantiating the fact that the compounds maintain the structural stability upon cycling. So, the maintenance of structural stability along with the (already mentioned) electrochemically size driven nano particle formation of these nitrides are believed to be responsible for the successively enhancing capacity values and the considerably reduced capacity fade upon cycling. However, a slight shift in the peak position observed for the $Si_{3-x}Fe_xN_4$ compound (Fig.6c) may be correlated with the gradually decreased specific capacity values exhibited by the compound upon extended cycling.

4. CONCLUSION

A series of novel category Si_3N_4 and $Si_{3-x}M_xN_4$ anodes containing M = Co, Ni, Fe has been synthesized and evaluated for electrochemical performance characteristics. All the compounds exhibited reversible electrochemical (intercalation/ de-intercalation) behavior with better cycleability and excellent coulumbic efficiency values individually. In particular, $Si_{3-x}Fe_xN_4$ anode showed the highest specific capacity, even after the expense of 50 cycles. On the other hand, silicon nitride (Si_3N_4) and the $Si_{3-x}M_xN_4$ [M=Co, Ni] derivatives showed better capacity retention upon extended cycling. Hence the present study recommends the series of Si_3N_4 and $Si_{3-x}M_xN_4$ compounds with M = Co, Ni, Fe as possible alternative anodes and more specifically, the $Si_{3-x}Fe_xN_4$ anodes for their high capacity capabilities to be exploited possibly in practical rechargeable lithium battery applications. Also, the study recommends the variety of Si_3N_4 and $Si_{3-x}M_xN_4$ [M=Co, Ni] compounds as potential anodes for better capacity retention.

References

1. M. Nishijima, T. Kagohashi, M. Imanishi, Y.Takeda, O.Yamamoto, S.Kondo, *Solid State Ionics*, 83 (1996) 107
2. M.Nishijima, Y,Takeda, N.Imanishi, O.Yamamoto, *J. Solid State Chem.*, 113 (1994) 205
3. M.Nishijima, N.Tadokoro, Y.Takeda, N.Imanishi,O.Yamamoto, *J.Electrochem.Soc.,* 141 (1994) 2966
4. M.Nishijima, Y.Takeda, M.Yamahata, K.Takeda,M.Imanishi,O.Yamamoto, *Solid State Ionics,* 130 (2000) 61
5. V.W.Sachsr, R.Juza, *Z.Anorg.Chem.*, 259 (1949) 278
6. T.Asai,K.Nishida,S.Kawai, *Mater.Res. Bull.*, 19 (1984) 1377
7. T.Shodai,S.Okada, S.Tohishima, J.Yamaki*, Solid State Ionics*, 86-88 (1996) 785
8. M.Nishijima, T. Kagohashi, Y.Takeda, M. Imanishi, O.Yamamoto*, J.Power Sources*, 68 (1997) 510
9. Y.M.Kang, S.C.Park, Y.S.Kanr, P.S.lee,J.Y.Lee, *Solid State Ionics*, 156 (2003) 263
10. M.F.Bell, A.Brietschwerdt, *Mater.Res.Bull.,* 16 (1981) 267
11. T.Lapp, S.Kaarup, A.Hooper, *Solid State Ionics*, 11 (1983) 97
12. N.Kalaiselvi,C.H.Doh, C.W.Park, B.S.Jin, S.I.Moon ,M.S.Yun, *Solid State Ionics*, (2004) 541
13. I.Kohatsu, J.W.McCauley, *Mater.Res.Bull.*, 9 (1974) 917
14. N.Kalaiselvi,C.H.Doh, C.W.Park, B.S.Jin, S.I.Moon ,M.S.Yun, *Private communication* (2004)
15. P.Poizot, S.Larulle,S.Grugeon, L.Dupont, J.M.Tarascon*, J.Power Sources*, 97-98 (2001) 235
16. Y.Takeda, J.Yang, N.Imanishi, *Solid State Ionics*, 152-153 (2002) 35